

Review of Computer Engineering Research

2023 Vol. 10, No. 4, pp. 136-149

ISSN(e): 2410-9142

ISSN(p): 2412-4281

DOI: 10.18488/76.v10i4.3533

© 2023 Conscientia Beam. All Rights Reserved.





Pneumonia and tuberculosis detection with chest x-ray images and medical records using deep learning techniques

 **Sudhir Kumar Mohapatra**¹⁺

 **Mesfin Abebe**²

 **Lidia Mekuanint**³

 **Srinivas Prasad**⁴

 **Prasanta Kumar Bala**⁵

 **Sunil Kumar Dhala**⁶

¹*Sri Sri University, India.*

¹*Email: sudhir.mohapatra@srisriuniversity.edu.in*

²*Email: sunildhal@srisriuniversity.edu.in*

³*Adama Science and Technology University, Ethiopia.*

³*Email: mesfinabha@gmail.com*

³*Email: tegegn1dita@gmail.com*

⁴*GITAM University, India.*

⁴*Email: sprasad@gitam.edu*

⁵*GITA Autonomous College, India.*

⁵*Email: prasanta_bal@yahoo.co.in*



(+ Corresponding author)

ABSTRACT

Article History

Received: 2 August 2023

Revised: 15 September 2023

Accepted: 6 October 2023

Published: 28 November 2023

Keywords

Chest x-ray image
Convolutional neural network
Deep learning
Medical records
Multilayer perceptron
Pneumonia
Tuberculosis.

Pneumonia and tuberculosis are the major public health problems worldwide. These diseases affect the lungs, and if they are not diagnosed properly in time, they can become a fatal health problem. Chest x-ray images are widely used to detect and diagnose Pneumonia and Tuberculosis disease. Detection of Pneumonia and Tuberculosis from chest x-ray images is difficult and requires experience due to the similar pathological features of the diseases. Sometimes a misdiagnosis of the disease occurs due to this similarity. Several researchers used deep learning and machine learning techniques to solve this misdiagnosis problem. However, these studies used the chest x-ray images only to develop Pneumonia and Tuberculosis disease detection models. But using the chest x-ray images alone cannot necessarily lead to accurate disease detection and classification. In the traditional or manual approach, medical records are required to support and correctly interpret the chest x-ray images in the appropriate clinical context. This study develops a multi-input Pneumonia and Tuberculosis detection model using chest x-ray images and medical records to follow the clinical procedure. The study applied a Convolutional Neural Network for the chest x-ray image data and a Multilayer perceptron for the medical record data to develop the models. We implemented feature-level concatenation to join the output feature vectors from the Convolutional Neural Network and a Multilayer perceptron for the development of the disease detection model. For the purpose of comparison, we also developed image-only and medical record-only models. Consequently, the image-only model gives an accuracy of 92.68%, the medical record-only model results in 98.72% accuracy, and the combined model accuracy is improved to 99.61%. In general, the study shows that the fusion of the chest x-ray and the medical records leads to better accuracy and is more similar to the clinical approach.

Contribution/Originality: This study aimed to create a multi-modal deep learning model for the detection of Pneumonia and Tuberculosis diseases, employing clinical methodologies. Various feature extraction techniques were employed to find the most significant features from both the images and the medical data.

1. INTRODUCTION

The occurrence of lung infection is attributed to the infiltration of the lungs by a substantial microorganism, such as a virus or bacteria, resulting in detrimental effects on the pulmonary system. Pneumonia and TB (tuberculosis) are significant global public health concerns that have a profound impact on pulmonary health.. According to a report from the World Health Organization (WHO), Tuberculosis (TB) is the second-top infectiously deadly disease next to Coronavirus Disease (COVID-19) and above Human Immunodeficiency Virus / Acquired Immunodeficiency Syndrome (HIV/AIDS). In 2020, 1.2 million people¹ comprising 214,000 people who are HIV positive, died from TB worldwide. The COVID-19 pandemic has made the number of deaths worse since 2019 as a result of TB risk factors like malnutrition and poverty [1]. It showed that in 2021 and 2022, the case would become more exacerbated. On top of this, developing countries cover more than 95% of the death cases [1]. Tuberculosis is one of the most critical public health problems in Ethiopia. For instance, in 2020, 151,000 TB incidences will be recorded.

In addition, TB treatment coverage is 71%, and the remaining 29% of TB cases were not diagnosed. The main causes of TB morbidity and mortality in Ethiopia are co-infections with other diseases like HIV/AIDS and a lack of access to early diagnosis² and treatment. Mnyambwa, et al. [2] identified that TB disease detection and diagnosis are the consequence of increased patient burden, a poor laboratory system, and a lack of skilled workers. This gap has to be addressed to achieve the Sustainable Development Goals (SDG) target of ending TB by 2030. Typically, the signs and symptoms of active TB disease may become moderate for months. This leads to delayed medical attention and an increased risk of spreading the bacteria to others. Typically, the signs and symptoms of active TB disease may become moderate for months. In the absence of proper treatment, almost all HIV-positive individuals with TB and 45% of HIV-negative individuals with TB will die.

Pneumonia is responsible for 14% of all deaths among children under the age of five. For example, 740,000 children died from pneumonia in 2019. People with pre-existing health problems and adults over the age of 65 are also at risk for pneumonia. The disease can affect either or both lungs. When a healthy individual breathes, the tiny air sacs named alveoli that make up the lungs fill with air. When a person with pneumonia breathes, fluid and pus accumulate in the alveoli, which reduces their ability to take in oxygen and makes breathing painful. Viruses, bacteria, or fungi are the causes of pneumonia. Bacterial and viral pneumonia are contagious, while fungal pneumonia is not contagious. Ethiopia is among the sub-Saharan African countries with the highest rate of pneumonia. Even though various cost-effective interventions, such as good nutrition and immunization, can prevent pneumonia deaths, delays in diagnosing pneumonia are a major factor in the deaths of children under five [3].

Different medical imaging techniques have been used for the diagnosis of Pneumonia and TB disease. But, due to their accessibility, low radiation dose, and ease of use [4-6], chest x-rays are widely used for Pneumonia and TB diagnosis and health monitoring [7]. Diagnosing Pneumonia and TB disease using a chest x-ray image is a difficult task and requires skillfulness and experience. Pneumonia and tuberculosis closely resemble each other on chest x-ray images [4, 8]. Due to this, misdiagnosis between the two diseases occurs more frequently than any other lung disease [9].

Researchers apply machine learning and deep learning techniques to develop Pneumonia and TB detection models. Convolutional Neural Network (CNN) and pretrained models are widely used to develop detection models using chest x-ray images. These deep learning models are considered to only use chest x-ray image data. The models cannot contextualize the chest x-ray image according to the patient's medical history and other medical information in the way medical experts do. To achieve a similar goal to that of the real practitioner, patient medical

¹ <https://www.who.int/news-room/fact-sheets/detail/tuberculosis>

history should be used in addition to the chest x-ray image [10]. In this study, deep learning is used to develop a Pneumonia and TB detection model from patient medical records and a chest x-ray image dataset.

2. LITERATURE REVIEW

Different studies are conducted on applying machine learning and deep learning techniques to improve the detection and diagnosis of pneumonia and tuberculosis. Ayan and Ünver [11] used the Xception and Vgg16 CNN models to develop a pneumonia detection model from chest x-rays. The reason for using these two models was that both Xception and Vgg16 have better performance weights on the ImageNet dataset. The accuracy of Vgg16 was 0.87% and Xception was 0.82%, but Xception exceeded Vgg16 in the detection of pneumonia cases. Rajpurkar, et al. [12] developed a model named CheXNet that can detect 14 diseases, including pneumonia, from chest x-ray images at a level that outperforms a radiologist's work. CheXNet is a 121-layered CNN that takes a chest x-ray image, gives the likelihood of pneumonia, and indicates portions of the image that are most suggestive of pneumonia. The performance of CheXNet exceeded the average performance of radiologists on the F1 score. The authors stated their limitations as using only the frontal chest x-ray images and being unable to include patient history in addition to chest x-ray images.

Verma, et al. [8] pointed out that pulmonary infectious diseases are difficult to diagnose [13] because they mimic each other. As a result of this, the patient will suffer from misdiagnosed treatment. A case of a patient with tuberculosis misdiagnosed as pneumonia that resulted in death is presented. This paper aimed to propose a framework to classify Pulmonary Tuberculosis (PTB), bacterial pneumonia, and viral pneumonia from chest x-ray images using image processing techniques. The Neural network classifier and Inception V3 were used for the analysis of images and image embedding, respectively. For training purposes, the Shenzhen chest x-ray dataset and the China dataset on pneumonia are used. Rescaling, rotation, width and height shift, shear range, zoom range, and horizontal flipping augmentation techniques are applied.

We came up with a new deep learning algorithm called VGG Data STN with CNN (VDSNet) to improve CNN's poor performance on rotated and tilted image orientations [14]. VDSNet combines CNN, Visual Geometry Group (VGG), data augmentation, and a spatial transformer network (STN). This work conducted binary classification using chest x-ray images and x-ray view position, records of gender, and the age of the patient. The developed model performed with a validation accuracy of 73%. In this work, no image augmentation technique is utilized. The use of patient age and gender attributes has improved the accuracy of the model. The model developed only detects whether the lung disease is found or not; it does not identify which lung disease is detected. Hooda, et al. [6] proposed a deep CNN-based method for TB detection from chest x-ray image data. The reason behind developing this study was that traditional Computer-Aided Design (CAD) systems use handcrafted features, but deep learning automatically extracts and learns the best features. A 19-layer simple deep CNN architecture has been developed. The proposed architecture consists of convolutional, Relu, Fully Connected (FC), and dropout layers. Chest x-ray images used in this work are taken from Shenzhen and Montgomery public datasets by reducing the dimensions to 224x224 size. A total of 800 chest x-ray images were used, of which 600 were for training and 200 were for validation. Adam, SDG, and momentum optimizers were compared, and the Adam optimizer outperformed, with overall accuracy and validation accuracy obtained of 94.73% and 82.09%, respectively.

Haloi, et al. [4] have developed a pneumonia and TB classification model by modifying the architecture of a 21-layered deep network for traffic sign classification [15]. The model developed is a 211-layered deep CNN model. The dataset used was a collection of four publicly available chest x-ray datasets. A partial attention mechanism was used on inception classifier feature maps. Disagreement values between the model and radiologists are used as feedback to optimize the network parameters. A pre-trained model on the chest x-ray 14 dataset and data augmentation are used to improve the performance of the model. Data augmentation techniques of random flips to the left or right, up or down, and changing the pixel values randomly are applied in this work. The performance of

this model exceeded that of CheXNet [12] in detecting pneumonia cases. Overexposed chest x-rays applied for the development of the model have affected its performance. The overlapping domain of pneumonia and tuberculosis is considered in this work; the model can identify a chest x-ray image that contains both pneumonia and tuberculosis pathological features. This model only uses x-ray images to detect pneumonia and TB; no associated medical history of the patient is used.

Khatibi, et al. [16] proposed a two-step automatic method of pneumonia and TB detection using a stacked ensemble classifier. In the first step of the model, the symptoms and demographic factors of 191 patients are imputed, and features are selected by using stacked ensemble classifiers; the first step classification is also performed here. On the second step, the chest x-ray reports and laboratory results from the first step are applied to the stacked classifier again. The ensemble classifiers applied are AdaBoost, random forest, and gradient boosting. Single classifiers like decision tree (DT), Support Vector Machine (SVM), linear regression, and K Nearest Neighbor (KNN) are also applied to compare their performance. Another aim of developing a two-step model is to save time waiting for laboratory results and radiographic reports, in which this work can first show the result based on demographic information and patient symptoms in the phase one output. In this study, the radiology reports are used instead of the radiology images. This makes the developed system dependent on the decisions made by the radiologists directly, and this leads to biased results and variation in the views of the radiologists.

The researcher used machine learning and deep learning for different disease detections, like tuberculosis, breast cancer, and brain tumors [17-21]. They used the chest X-ray (CXR) images as input to the model and finally classified the image as infected or not infected.

3. DATA COLLECTION AND METHODOLOGY

The pneumonia and TB detection model combines chest x-ray images and medical record data to minimise the misdiagnosis problems that stem from models developed using chest x-ray images only or medical record data only. The main beneficiaries of this study are radiologists or medical doctors. The model aids radiologists or medical doctors in detecting pneumonia and TB in a more accurate way. This study incorporates 17 features of medical records along with chest x-ray images for the prediction of pneumonia and TB disease. We applied a multilayer perceptron to process the medical record data, and a convolutional neural network was applied to process the chest x-ray images. Then, the outputs of the two algorithms were merged together using the concatenation layers. The accuracy achieved in this study is 99.61%, which shows the proposed model can be used in the detection of pneumonia and TB cases.

3.1. Data Set Preparation

In this study, we have used locally collated datasets: medical records and chest x-ray images. The datasets are collected from three local hospitals in Ethiopia: Alert Hospital, St Peter's Specialized Hospital, and Yekatit 12 Hospital Medical College. A total of 2,931 chest x-ray images and medical records were collected from the three hospitals, as shown in Table 1.

Table 1. Local data sources.

Disease type	Alert Hospital	St. Peter's Hospital	Yekatit 12 Hospital	Total
Pneumonia	152	489	391	1,032
TB	176	397	341	914
Other	154	463	368	985
Total	482	1,349	1,100	2,931

The chest x-ray images are cleaned from texts using the Keras Optical Character Recognition (OCR) library, which is shown in Figure 1. We loaded a batch size of images for the Keras OCR to clean. The images are loaded from the drive according to their path in a csv file. The OCR checks every part of the image, pixel by pixel, and

removes the text found on the image. The image is converted to Red, Green, and Blue (RGB) format to avoid color inversion. Furthermore, the Chest x-ray images are converted to greyscale, and augmentation techniques are applied. All images are resized to 512 x 512 sizes, and normalization is also performed. In this study, we have performed seven types of augmentation techniques to do seven different experiments on the performance of the model with respect to the augmentation techniques applied, as shown in Table 4.

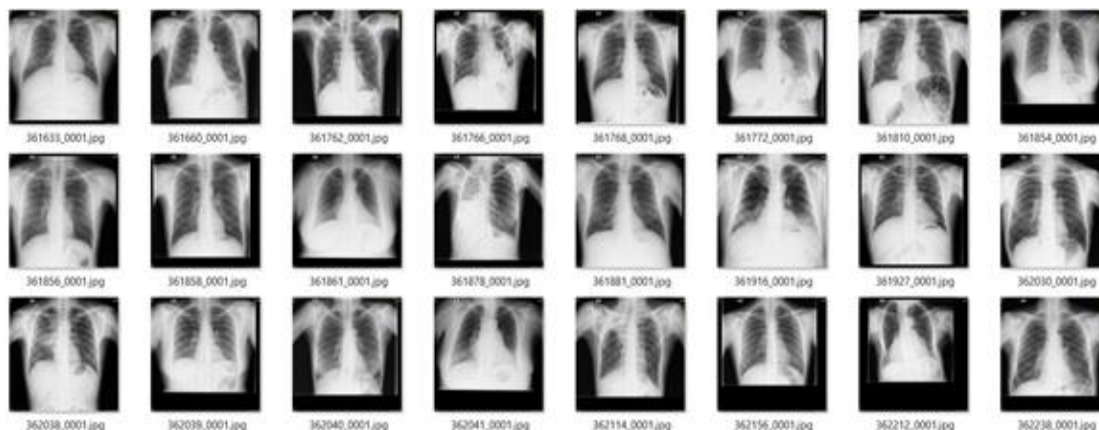


Figure 1. Sample chest X-ray images before preprocessing.

3.2. Deep Learning Techniques and Feature Selection

Deep learning is the part of machine learning that needs a high quantity of data to learn from and get better accuracy than the traditional machine learning algorithms. Deep learning classification techniques can also produce numerical outputs between 0 and 1, but classification algorithms in traditional machine learning approaches are only considered to be either 0 or 1 [22]. In this study, we used a Convolutional neural network for the processing of chest x-ray image data. CNN network is a deep learning algorithm for processing data with a grid pattern that is inspired by the organization of the animal visual cortex and meant to learn spatial hierarchies of features from low-level to high-level patterns. CNNs are the most effective neural networks for computer vision tasks such as image recognition and classification. The convolution layer, pooling layer, and fully connected layers are the building blocks of CNN [23]. A crucial component of the CNN design is the convolution layer, which combines linear and nonlinear methods, such as activation functions and convolution, to conduct feature extraction. In order to limit the number of trainable parameters and establish translation invariance to minute shifts and distortions, a pooling layer samples the feature maps. This minimizes their in-plane dimensionality. It is the convolution or pooling layer's output feature maps that are flattened and turned into a one-dimensional array. These are then linked to other fully connected layers in the Fully Connected Layer (Dense Layer), where a learnable weight connects each input to each output. Machine learning algorithms perform well on tabular data, but in order to make them suitable for model concatenation and deployment, we preferred using neural networks [24]. A multi-layer perceptron is a type of artificial neural network that can be used for classification and regression tasks. Due to its simplicity, good performance on tabular datasets, and good achievements in the medical field [25]. Multilayer Perceptron (MLP) is used to process the tabular medical record dataset in this study, which is shown in Table 2.

We applied the Random forest classifier algorithm for the feature selection task in the medical record dataset. By adding bootstrap aggregation and randomization methods to the decision tree classifier while it is being built, random forest classifiers make the single tree better at classifying [26]. Gini impurity, or information gain, is used as a measure of impurity. Features with lower impurity levels are important, and vice versa. Our medical record dataset contains both categorical and continuous independent variables, and random forest classifiers can handle both well. We have used random forest classifiers because of their high accuracy, better generalization, and interpretability.

Table 2. Sample medical record dataset.

	Age	Sex	Temp	RR	PR	Cough_D	Cough_T	me	CP	SOB	SP02	Fever	NS	HTB	Contact	HS	WL	HIV	Diagnosis	IMG
2646	35.0	M	38.8	30.0	81	4.30	yellowish	11.50	Yes	Yes	90.0	Low	Yes	No	No	No	Yes	p	TB	lb (573).png
874	65.0	M	36.0	16.0	95	0.14	dry	11.00	No	No	95.0	No	No	No	No	No	No	N	Other	Other (875).png
1794	0.3	M	36.5	32.0	110	0.42	dry	8.37	Yes	Yes	100.0	High	No	No	No	No	No	N	Pneumonia	Pneumonia (795).png
297	86.0	M	37.0	20.0	77	0.14	dry	10.00	No	No	99.0	No	No	No	No	No	No	N	Other	Other (298).png
1076	55.0	M	36.5	30.0	114	2.00	whitish	8.37	Yes	Yes	93.0	High	No	No	No	No	No	N	Pneumonia	Pneumonia (77).png

3.3. Proposed Approach

The study is performed to predict pneumonia and TB disease by using a medical record dataset and a chest x-ray image dataset. Figure 2 shows the overall process of the proposed approach. In the first step, the two data sets are preprocessed according to their unique nature (structural data, image). In the second step, the preprocessed chest x-ray image and medical record datasets are processed according to the architecture proposed below. The medical record dataset is processed using a multilayer perceptron, and the chest x-ray image is also processed using a convolutional neural network. By taking the feature vector outputs from the two algorithms, the processed features are concatenated.

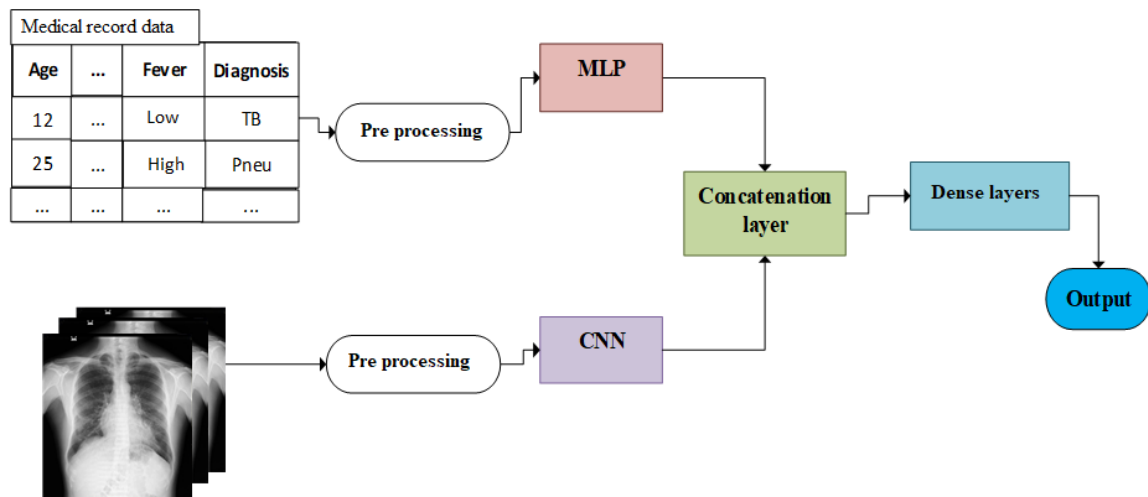


Figure 2. Proposed X-ray image and medical recorded data approach.

4. EXPERIMENTAL RESULTS

The implementation part is done in the Google Colab Pro environment. Google Colab Pro provides a large Random Access Memory (RAM) size of 25.46GB, faster Graphics Processing Units (GPU), and more usage time than the free version. Accuracy, F1-Score, precision, and recall evaluation metrics are used to measure the performance of the models, as shown in Table 6.

4.1. Medical Record Preprocessing

The medical record dataset contains 2931 rows with 18 columns and was later reduced to 17 columns. We performed different preprocessing techniques to make the dataset ready for model building. The dataset features, along with their data types, are presented in Table 3.

4.1.1. Data Cleaning on the Medical Recorded Dataset

4.1.1.1. Unit Conversion

We converted different units from one unit value to another unit value. In the age column, the ages of children below age one (1) are recorded in months. Such records are converted to years by dividing the month by 12. The cough duration of patients is also recorded by days, weeks, months, and years. Days, months, and years are converted to weeks. We have checked the outliers, and the outliers have been removed.

4.1.1.2. Data Transformation

We transform the medical record dataset into the categorical features that are shown in Table 3. We apply categorical encoding, label encoding, and one-hot encoding data transformation techniques.

- *Ordinal encoding*: we applied ordinal encoding to categorical data types that have ordered relationships. Example: Cough type and fever.
- *Label encoding*: is applied to encode categorical values that do not have an ordered relationship, such as sex, chest pain, and shortness of breath, night sweat, and history of tuberculosis, contact with a chronic cougher, history of smoking, weight loss, and HIV test results.
- *One hot encoding*: is used to encode each output value into a new column by creating dummy variables.

Table 3. Features with their data types.

Feature	Symbol	Data type
Age	Age	Continuous
Sex	Sex	Categorical(Nominal) M – 0 F – 1
Temperature	Temp	Continuous
Respiratory rate	RR	Continuous
Pulse rate	PR	Continuous
Cough duration in weeks	Cough_D	Continuous
Cough type	Cough_T	Categorical(Ordinal) 0- dry 1-whitish 2- yellowish 3-bloody
White blood cell count	WBC	Continuous
Chest pain	CP	Categorical(Nominal) 0 – no 1 – yes
Shortness of breath	SOB	Categorical(Nominal) 0 – no 1 – yes
Oxygen saturation	SPO ₂	Continuous
Fever	Fever	Categorical(Ordinal) 0 – no 1 – low 2 – high
Night sweat	NS	Categorical(Nominal) 0 – no 1 – yes
History of TB	HTB	Categorical(Nominal) 0 – no 1 – yes
Contact with chronic cougher	Contact	Categorical(Nominal) 0 – no 1 – yes
History of smoking	HS	Categorical(Nominal) 0 – no 1 – yes
Weight loss	WL	Categorical(Nominal) 0 – no 1 – yes
HIV test result	HIV	Categorical(Nominal) 0 – P 1 – N
Diagnosis	Diagnosis	Categorical(Nominal) 0 – other 1 - pneumonia 2 - TB

4.1.2. Data Normalization

Data normalization allows the values to have a common scale without distorting the variations in values. We perform the normalization technique by using the absolute maximum scaler technique for columns having values greater than 1. Normalization techniques are used based on age, temperature, respiratory rate, pulse rate, cough duration, white blood cell count, oxygen saturation, fever, and cough type. After normalization, every value scales between 0 and 1.

4.2. Feature Selection

After the data was cleaned, we employed feature selection to select features that contributed to improving the model's performance. The random forest classifier is used to identify the relevant features and to use those features for the model building process, as shown in Figure 3.

4.3. Image Preprocessing Techniques

The collected chest x-ray images are RGB images with 3 channels. These images are converted to greyscale to minimize the complexity and reduce computational resource requirements. In image preprocessing, image cleaning and image augmentation techniques are applied to the chest x-ray images. Meta information on the local chest x-ray images is cleaned using OCR, and then image augmentation is performed.

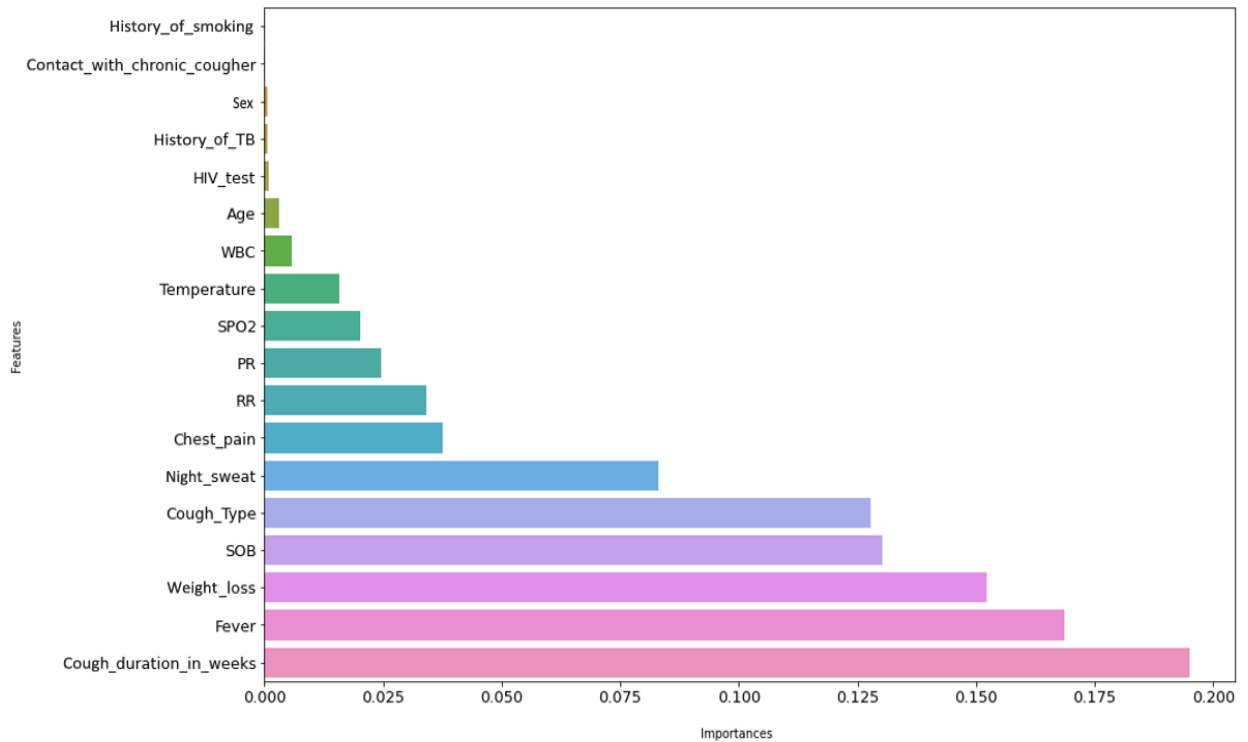


Figure 3. Feature selection result.

After cleaning, image augmentation techniques are applied to the chest x-ray images. According to Sirazitdinov, et al. [26], rotation, horizontal flip, and random brightness augmentation techniques applied to chest x-ray images have shown better performance gains on the model, as indicated in Table 4. Rotation between -5 and 5 , equal scaling in the x and y axis, and translation (height shift and width shift) are stated as medically recommended augmentation techniques, and horizontal flip is not recommended medically because it can lead to a non-physiological image [27]. Pivoting from these two papers, we selected rotation between -5 and 5 , random brightness, height shift, and width shift augmentation techniques to perform on our chest x-ray image dataset. We apply image augmentation to only get varying versions of the original dataset without increasing the dataset size. We do not increase the size of the dataset because the number of chest x-ray images and medical record rows should not be equal to the concatenation.

Table 4. Data augmentation techniques and model accuracy.

Experiment	Grey scaling	Brightness	Rotation	Height shift	Width shift	Accuracy (%)
1	X					98.77
2		X		X	X	98.70
3		X		X		98.87
4		X	X			98.98
5		X	X	X	X	98.94
6			X	X	X	98.98
7			X		X	99.08

4.4. Concatenation Layer

We defined a concatenation layer to concatenate the output feature vectors of CNN and MLP. The length of the features from CNN and MLP can be equal or not. But the number of datasets of medical records and chest x-ray images should be equal. Because concatenation concatenates the features of a single data row to the corresponding chest x-ray image features found at the same index position. In other words, the medical record information of a single person becomes concatenated with the associated single chest x-ray image. No medical record of a single

person can be joined with another chest x-ray image with a different index position. There is a one-to-one correspondence between the two datasets.

5. RESULTS OF THE STUDY

For comparison purposes, we have also developed image-only and medical record-only models. We used CNN and MLP sequential models, respectively. To develop the image-only model, a similar number of neurons and layers as the CNN of the functional model is used. We also applied L2 regularization to increase the performance of the model. The Adam optimizer with a learning rate of 0.0001 is applied. The LeakyReLU activation function is also used in the hidden layer of the model. To develop the MLP-only sequential model and the CNN-only sequential model, we used similar layers as in the MLP and CNN of the functional model. The results of the MLP-only model and CNN-only model confusion matrix are shown below in Figure 4a and Figure 4b.

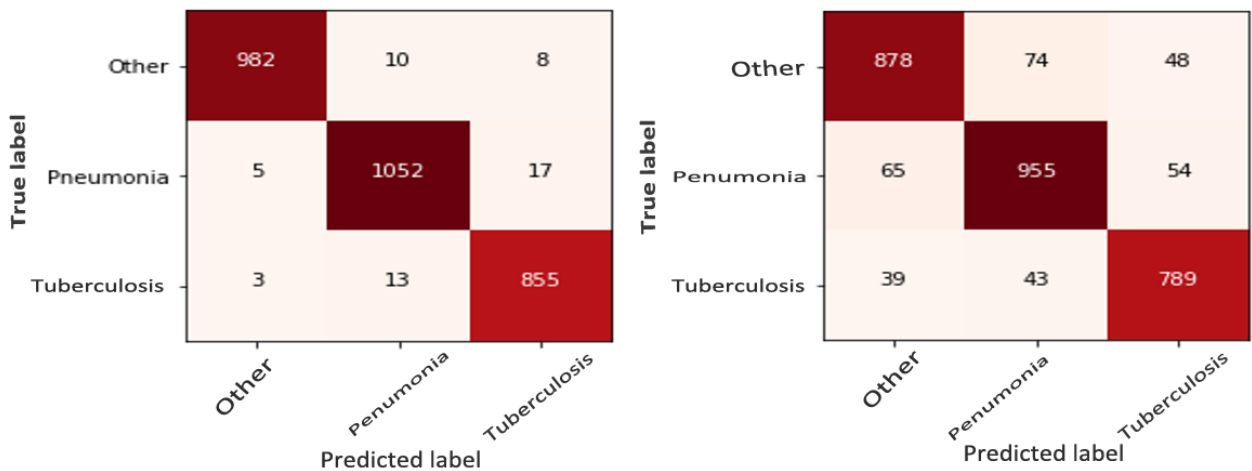


Figure 4. MLP (a) and CNN (b) sequential model confusion matrix results respectively.

Table 5. Comparison of the three models.

Developed model	MLP only model	CNN only model	MLP+CNN model
Accuracy (%)	98.72	92.68	99.61

As shown in Table 5, the performance of the joint model exceeded that of the single models of image and medical record. In addition, Table 6 shows the accuracy of the proposed model with respect to the three classes (pneumonia, TB, and others) of the dataset.

Table 6. Accuracy of validation methods.

Class	Precision (%)	Recall (%)	F1-score (%)	Accuracy (%)
Pneumonia	99.07	99.44	99.25	99.52
TB	99.53	99.19	99.35	99.62
Other	99.69	99.4	99.54	99.69
Average accuracy				99.61

The training and validation accuracy and loss graph of the joint model trained on 10 folds is shown in Figure 5. The confusion matrix of the joint model is shown in Figure 6.

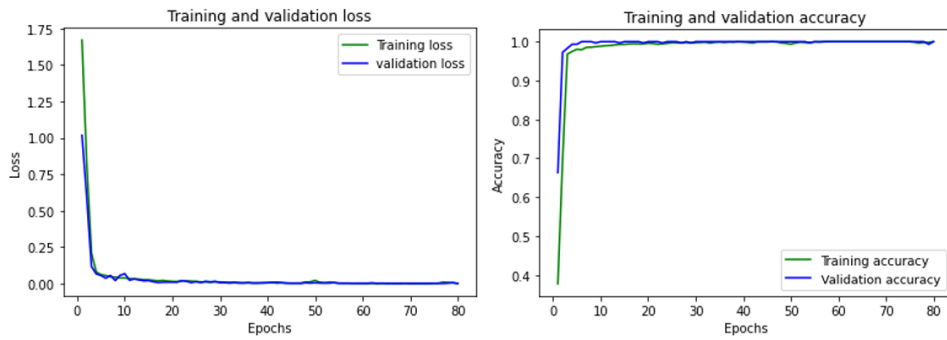


Figure 5. Accuracy and loss curve results for K=10.

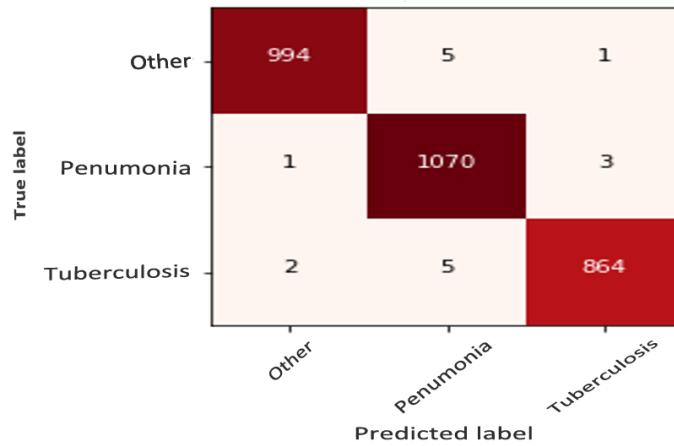


Figure 6. Developed joint model confusion matrix result.

6. DISCUSSION

Previous works that applied deep learning to develop pulmonary disease detection models [4, 6, 8, 11, 12] applied only chest x-ray images to develop detection models. These studies missed the right medical diagnosis procedure of including the patient's medical history for proper disease detection from chest x-ray images. Khatibi, et al. [16], who applied machine learning techniques to detect pneumonia and TB from patient symptoms and radiology reports, found that the models' performance is highly dependent on the decision made by the radiologist on the chest x-ray image. In other words, the algorithms do not directly detect the medical images, which leads to bias. Even though the work of Bharati, et al. [14] tried to use patient age, gender, and view position of the image information in addition to the chest x-ray image, this work failed to detect the specific disease; rather, it only shows whether the disease is detected or not. Therefore, the first aim of this study is to develop a pneumonia and TB model by incorporating patient medical records and chest x-ray images together. The detection enables the identification of pneumonia and TB disease.

Table 7. Hyper parameters combination for tuning.

Task	Dropout	Batch size	Epoch	Activation function	Learning rate	Kernel size	Acc (%)	F1-score (%)
1	0.25	32	100	Relu	0.001	3x3	99.36	99.03
2	0.1	60	50	Relu	0.001	3x3	99.40	99.11
3	0.5	40	60	Relu	0.01	5x5	99.27	98.97
4	0.1	30	50	LeakyReLU	0.001	5x5	99.25	98.87
5	0.25	40	80	Relu	0.001	7x7	99.49	99.24
6	0.2	30	60	LeakyReLU	0.001	3x3	95.58	93.42
7	0.1	30	50	Relu	0.001	7x7	99.29	98.97
8	0.5	30	60	LeakyReLU	0.001	7x7	99.33	99.00
9	0.25	40	80	Relu	0.001	5x5	99.43	99.14
10	0.25	40	80	Relu	0.001	3x3	99.27	98.90

Hyper-parameter tuning is done to improve the accuracy of the model. We have performed hyper-parameter tuning to minimize training time and remove unnecessary parameters. We have performed the hyper-parameter tuning using manual techniques. The various parameters used during the tuning process and the results achieved are shown in Table 7. By applying 10 different combinations of hyper-parameters, we have shown average accuracy and an average F1 score in the above table. The combination indicated in task 5 has shown slightly higher performance than the other combinations. Therefore, we have nominated the combination of hyper-parameters indicated in task 5, dropout of 0.25, batch size of 40, 80 epochs, relu activation function, learning rate of 0.0001, and kernel size of 7x7 to develop the final model. The selected combination is used to develop our pulmonary infectious disease detection model.

One way of improving the performance of the algorithms is by using k-fold cross-validation. We fed the preprocessed chest x-ray image and Medical record to the algorithms and trained those using different K fold values. The model gives the best accuracy when k=10 as shown in Table 8. We have gotten better average accuracy on this training than 3 and 5 folds.

Table 8. Classification result based on the three classes.

Class	Precision (%)	Recall (%)	F1-score (%)	Accuracy (%)
Pneumonia	99.07	99.44	99.25	99.52
TB	99.53	99.19	98.35	99.62
Other	99.69	99.40	99.54	99.69
Average accuracy				99.61

To the best of our knowledge, no model has been created to identify pneumonia and tuberculosis (TB) based on chest x-ray pictures and medical records that go beyond the patient's age and gender. We have made use of local chest x-ray pictures and our own dataset of medical information. As such, direct comparisons of this work with other studies on pneumonia and tuberculosis disease detection models are not possible.

7. CONCLUSION

This paper presents the development of a disease detection model for pneumonia and tuberculosis utilizing chest x-ray images and medical information. In order to attain our objective, we have undertaken many procedures, including data pretreatment, feature selection, and picture augmentation. Convolutional neural networks and multilayer perceptron's are among the deep learning methods that have been employed in this study. The feature vectors produced by both methods are combined using feature-level concatenation. Comparing models that only use images or medical records shows that models that combine medical records and chest x-ray images work better than models that only use medical records. The present work holds significant importance within the medical domain as it closely emulates the process by which radiologists analyze and reach conclusions regarding the visual characteristics of chest x-ray pictures in practical medical diagnostic settings. This study's findings provide valuable assistance to medical professionals, namely radiologists, in effectively and promptly identifying diseases through the analysis of chest x-ray pictures and medical data. The patients are also recipients of the findings of this study, as it enables them to receive a timely and precise diagnosis of the disease. The created model effectively addresses the issue of inaccuracies observed in models that just rely on chest x-ray images or medical data. In order to enhance the representativeness of the models, it is advisable to use a greater volume of local medical records and chest x-ray pictures obtained from diverse institutions in future studies. This is particularly relevant given the varying stages and types of tuberculosis (TB) disease.

Funding: This study received no specific financial support.

Institutional Review Board Statement: Not applicable.

Transparency: The authors state that the manuscript is honest, truthful, and transparent, that no key aspects of the investigation have been omitted, and that any differences from the study as planned have been clarified. This study followed all writing ethics.

Competing Interests: The authors declare that they have no competing interests.

Authors' Contributions: Conceptualization, M.A.; methodology and investigation, L.M.; formal analysis and writing, M.A and L.M.; resources, S.K.M. and S.K.D.; data curation, P.K.B. and S.P.; writing, review and editing, S.K.M.; visualization, P.K.B. and S.K.D.; supervision, S.K.M., S.P.; funding acquisition, S.K.D. All authors have read and agreed to the published version of the manuscript.

REFERENCES

- [1] Global Tuberculosis Report, "Global tuberculosis report," Retrieved: <https://apps.who.int/iris/rest/bitstreams/1379788/retrieve>. 2021.
- [2] N. P. Mnyambwa *et al.*, "Gaps related to screening and diagnosis of tuberculosis in care cascade in selected health facilities in East Africa countries: A retrospective study," *Journal of Clinical Tuberculosis and Other Mycobacterial Diseases*, vol. 25, p. 100278, 2021. <https://doi.org/10.1016/j.jctube.2021.100278>
- [3] B. B. Abate, A. M. Kasie, M. A. Reta, and M. W. Kassaw, "Neonatal sepsis and its associated factors in East Africa: A systematic review and meta-analysis," *International Journal of Public Health*, vol. 65, no. 9, pp. 1623-1633, 2020. <https://doi.org/10.1007/s00038-020-01489-x>
- [4] M. Haloi, K. R. Rajalakshmi, and P. Walia, "Towards radiologist-level accurate deep learning system for pulmonary screening," *arXiv preprint arXiv:1807.03120*, 2018.
- [5] C. Qin, D. Yao, Y. Shi, and Z. Song, "Computer-aided detection in chest radiography based on artificial intelligence: A survey," *Biomedical Engineering Online*, vol. 17, no. 1, pp. 1-23, 2018. <https://doi.org/10.1186/s12938-018-0544-y>
- [6] R. Hooda, S. Sofat, S. Kaur, A. Mittal, and F. Meriaudeau, "Deep-learning: A potential method for tuberculosis detection using chest radiography," in *2017 IEEE International Conference on Signal and Image Processing Applications (ICSIPA)*, 2017: IEEE, pp. 497-502.
- [7] S. Stirenko *et al.*, "Chest X-ray analysis of tuberculosis by deep learning with segmentation and augmentation," in *2018 IEEE 38th International Conference on Electronics and Nanotechnology (ELNANO)*, 2018: IEEE, pp. 422-428.
- [8] D. Verma, C. Bose, N. Tufchi, K. Pant, V. Tripathi, and A. Thapliyal, "An efficient framework for identification of tuberculosis and Pneumonia in chest X-ray images using neural network," *Procedia Computer Science*, vol. 171, pp. 217-224, 2020. <https://doi.org/10.1016/j.procs.2020.04.023>
- [9] M. Park *et al.*, "Distinguishing nontuberculous mycobacterial lung disease and Mycobacterium tuberculosis lung disease on X-ray images using deep transfer learning," *BMC Infectious Diseases*, vol. 23, no. 1, pp. 1-11, 2023.
- [10] S.-C. Huang, A. Pareek, S. Seyyedi, I. Banerjee, and M. P. Lungren, "Fusion of medical imaging and electronic health records using deep learning: A systematic review and implementation guidelines," *NPJ Digital Medicine*, vol. 3, no. 1, p. 136, 2020. <https://doi.org/10.1038/s41746-020-00341-z>
- [11] E. Ayan and H. M. Ünver, "Diagnosis of pneumonia from chest X-ray images using deep learning," in *2019 Scientific Meeting on Electrical-Electronics & Biomedical Engineering and Computer Science (EBBT)*, 2019: IEEE, pp. 1-5.
- [12] P. Rajpurkar *et al.*, "Chexnet: Radiologist-level pneumonia detection on chest x-rays with deep learning," *arXiv preprint arXiv:1711.05225*, 2017.
- [13] T. Rahman *et al.*, "Reliable tuberculosis detection using chest X-ray with deep learning, segmentation and visualization," *IEEE Access*, vol. 8, pp. 191586-191601, 2020. <https://doi.org/10.1109/access.2020.3031384>
- [14] S. Bharati, P. Podder, and M. R. H. Mondal, "Hybrid deep learning for detecting lung diseases from X-ray images," *Informatics in Medicine Unlocked*, vol. 20, p. 100391, 2020. <https://doi.org/10.1016/j.imu.2020.100391>
- [15] M. Haloi, "Traffic sign classification using deep inception based convolutional networks," *arXiv preprint arXiv:1511.02992*, pp. 11-15, 2015.

- [16] T. Khatibi, A. Farahani, and H. Sarmadian, "Proposing a two-step decision support system (TPIS) based on stacked ensemble classifier for early and low cost (step-1) and final (step-2) differential diagnosis of mycobacterium tuberculosis from non-tuberculosis Pneumonia," *arXive-prints*, 2020.
- [17] B. Debata, S. K. Mohapatra, and R. Priyadarshini, "A Systematic literature review on pulmonary disease detection using machine learning," in *Proceedings of the International Conference on Cognitive and Intelligent Computing: ICCIC 2021*, 2023, vol. 2: Springer, pp. 515-522.
- [18] S. K. Mohapatra, B. G. Assefa, and G. Belayneh, "A SVM based model for COVID detection using CXR image," in *Advances of Science and Technology: 9th EAI International Conference, ICAST 2021, Hybrid Event, Bahir Dar, Ethiopia, August 27-29, 2021, Proceedings, Part I*, 2022: Springer, pp. 368-381.
- [19] S. K. Mohapatra, *Automatic lung Tuberculosis detection model using thorax radiography image. In Deep Learning Applications in Medical Imaging*. IGI Global, 2021, pp. 223-242.
- [20] A. A. Mekonnen, H. W. Seid, S. K. Mohapatra, and S. Prasad, *Developing brain tumor detection model using deep feature extraction via transfer learning. In Handbook of Research on Automated Feature Engineering and Advanced Applications in Data Science*. IGI Global, 2021, pp. 119-137.
- [21] M. W. Walle, K. K. Tune, N. T. Sinshaw, and S. K. Mohapatra, "Transfer learning based breast cancer classification via deep convolutional neural network," *International Journal of Engineering and Manufacturing*, vol. 13, no. 4, pp. 34-43, 2023.
- [22] F. Ertam and G. Aydın, "Data classification with deep learning using Tensorflow," in *2017 International Conference on Computer Science and Engineering (UBMK)*, 2017: IEEE, pp. 755-758.
- [23] A. Patil and M. Rane, "Convolutional neural networks: An overview and its applications in pattern recognition," *Information and Communication Technology for Intelligent Systems: Proceedings of ICTIS 2020*, vol. 1, pp. 21-30, 2021.
- [24] A. Kadra, M. Lindauer, F. Hutter, and J. Grabocka, "Well-tuned simple nets excel on tabular datasets," *Advances in Neural Information Processing Systems*, vol. 34, pp. 23928-23941, 2021.
- [25] C. Dangare and S. Apte, "A data mining approach for prediction of heart disease using neural networks," *International Journal of Computer Engineering and Technology*, vol. 3, no. 3, pp. 30-40, 2012.
- [26] I. Sirazitdinov, M. Kholiavchenko, R. Kuleev, and B. Ibragimov, "Data augmentation for chest pathologies classification," in *2019 IEEE 16th International Symposium on Biomedical Imaging (ISBI 2019)*, 2019: IEEE, pp. 1216-1219.
- [27] M. Elgendi *et al.*, "The effectiveness of image augmentation in deep learning networks for detecting COVID-19: A geometric transformation perspective," *Frontiers in Medicine*, vol. 8, p. 629134, 2021. <https://doi.org/10.3389/fmed.2021.629134>

Views and opinions expressed in this article are the views and opinions of the author(s), Review of Computer Engineering Research shall not be responsible or answerable for any loss, damage or liability etc. caused in relation to/ arising out of the use of the content.